Surface solitons in two-dimensional chirped photonic lattices

Mario I. Molina[1,2,3], Yaroslav V. Kartashov[2], Lluis Torner[2], and Yuri S. Kivshar[3]

[1] *Departamento de Física, Facultad de Ciencias,*
Universidad de Chile, Santiago, Chile

[2] *ICFO-Institut de Ciencies Fotoniques,*
and Universitat Politecnica de Catalunya,
Mediterranean Technology Park, 08860 Castelldefels (Barcelona), Spain

[3] *Nonlinear Physics Center, Research School of Physical Sciences and Engineering,*
Australian National University, Canberra, ACT 0200, Australia

Abstract

We study surface modes in semi-infinite chirped two-dimensional photonic lattices in the framework of an effective discrete nonlinear model. We demonstrate that the lattice chirp can change dramatically the conditions for the mode localization near the surface, and we find numerically the families of surface modes, in linear lattices, and discrete surface solitons, in nonlinear lattices. We demonstrate that, in a sharp contrast to one-dimensional discrete surface solitons, in two-dimensional lattices the mode threshold power is lowered by the action of both the surface and lattice chirp. By manipulating with the lattice chirp, we can control the mode position and its localization.

PACS numbers: 42.65.-k, 42.65.Tg, 42.65.Wi

I. INTRODUCTION

In linear guided-wave optics surface states have been predicted to exist at interfaces separating periodic and homogeneous dielectric media [1]. The interest in the study of surface states has been renewed recently because an interplay of self-focusing nonlinearity and repulsive effect of the surface was shown to facilitate the formation of discrete surface solitons located at the edge of the waveguide array [2, 3]. These surface solitons can be understood as discrete optical solitons localized near the surface provided their power exceeds a certain threshold value, compensating the repulsive action of the surface [4]. A similar effect of the light localization near the edge of the waveguide array and the formation of surface gap solitons have been predicted and observed for defocusing nonlinear periodic media [2, 5, 6, 7].

In recent studies [8], it was demonstrated that the conditions for the soliton formation can be dramatically modified near the surface of a chirped optical lattice. It was found that, due to combined actions of internal reflection at the interface, distributed Bragg-type reflection and focusing nonlinearity, surfaces of chirped lattices become soliton attractors, in a sharp contrast with the standard lattices. The main conclusions of those studies have been confirmed later by employing a discrete model [9].

It is important to analyze how the properties of nonlinear surface waves are modified by the lattice dimensionality, and the first studies of different types of discrete surface solitons in two-dimensional nonlinear photonic lattices [10, 11, 12, 13, 14] revealed, in particular, that the presence of a surface increases the stability region for two-dimensional (2D) discrete solitons [13] and the threshold power for the edge surface state is slightly higher than that for the corner soliton [12, 14]. Recent observations of two-dimensional surface solitons in optically-induced photonic lattices [15] and laser-written waveguide arrays in fused silica [16] demonstrated novel features of these nonlinear surface modes in comparison with their counterparts in one-dimensional waveguide arrays.

In this paper, we employ a two-dimensional discrete model of a chirped photonic lattice to provide a deeper physical insight into the properties of linear surface modes and discrete surface solitons in two-dimensional chirped photonic lattices. In particular, we demonstrate that there appears a critical value of the lattice chirp for the existence of a linear mode localized at the surface such that above this critical value the surface solitons originate from

the corresponding linear surface modes, and they do not require any threshold power for their existence. We study the dependence of the mode position near the surface and the critical power as a function of the lattice chirp, and also demonstrate how the engineered chirp of the photonic lattice can facilitate a selective nonlinear localization near the surface.

The paper is organized as follows. In Sec. II we introduce our discrete nonlinear model of a two-dimensional chirped lattice. Section III is devoted to the study of localized modes in linear chirped lattices. In particular, we consider two special cases of the chirp and demonstrate that the chirp can change dramatically the conditions for the mode localization near the surface, so that surface modes may exist even in a linear lattice provided the chirp parameter exceeds some threshold value. In Sec. IV we study the localization of nonlinear modes near the surface and, in particular, demonstrate that by engineering the lattice chirp we can control the localization of nonlinear modes and their location on the lattice. Finally, Sec. V concludes the paper.

II. MODEL

We consider a two-dimensional array of $N \times N$ nonlinear (Kerr) single-mode waveguides which form a square lattice with the lattice spacing $a(\equiv 1)$. We introduce a spatial chirp into the system by either changing the individual refraction index of the guides and/or adjusting the waveguide spacings. In the first case, both the propagation constant and coupling between the neighboring waveguides become chirped; in the second case, only the coupling is affected. In particular, it is possible to have a situation where the coupling chirp is greatly reduced by compensating a change in the refraction index by a judicious change of the waveguide distance. As a result, only chirp in the propagation constant is relevant in this case. In what follows we consider both the cases separately since they do lead to a different asymptotic behavior.

In the framework of the coupled-mode theory, the nonlinear equations for the amplitudes of the stationary modes can be written in general as

$$-\beta C_{\mathbf{n}} + \lambda_{\mathbf{n}} C_{\mathbf{n}} + \sum_{\mathbf{m}} V_{\mathbf{n},\mathbf{m}}\, C_{\mathbf{m}} + \gamma |C_{\mathbf{n}}|^2 C_{\mathbf{n}} = 0 \tag{1}$$

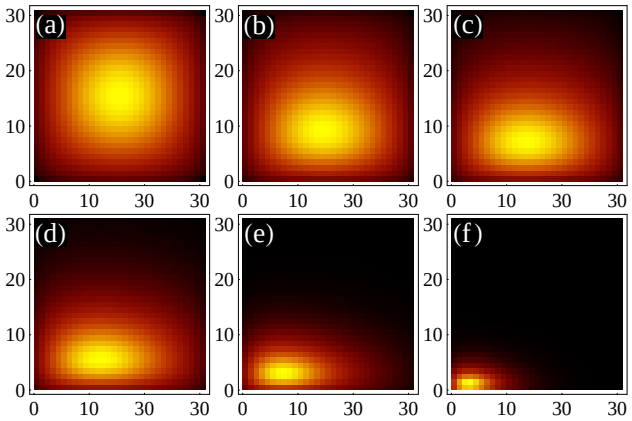

FIG. 1: Density profiles of localized nodeless modes for different values of the chirp (σ_x, σ_y) for a 31×31 linear array with $\lambda_0/V_0 = 5$. (a): $(0,0)$, (b) $(5 \times 10^{-5}, 5 \times 10^{-4})$, (c) $(10^{-4}, 10^{-3})$, (d) $(2 \times 10^{-4}, 2 \times 10^{-3})$, (e) $(10^{-3}, 10^{-2})$, (f) $(10^{-2}, 10^{-1})$. Anisotropic chirp in the propagation constant.

For a two-dimensional semi-infinite square nonlinear lattice, Eq.(1) becomes

$$\begin{aligned} &-\beta C_{n,m} + \lambda_{n,m} C_{n,m} + \sum_{j=\pm 1} V_{(n,m),(n+j,m)} C_{n+j,m} \\ &+ \sum_{j=\pm 1} V_{(n,m),(n,m+j)} C_{n,m+j} + \gamma |C_{n,m}|^2 C_{n,m} = 0, \end{aligned} \tag{2}$$

where $n \geq 0$ and $m \geq 0$, and $V_{(n,m),(n',m')} = 0$ if either $n' < 0$ or $m' < 0$.

We now modulate the refraction index $\rho(n,m)$ of each guide to decrease it exponentially away from the corner site $(0,0)$, in a general, anisotropic manner:

$$\rho(n,m) = \rho_0 \exp(-\sigma_x n - \sigma_y m),$$

where σ_x and σ_y are two chirp parameters in the x and y-direction, respectively. This change in the refraction index affects the effective propagation constant of each guide in a similar way,

$$\lambda_{n,m} = \lambda_0 \exp(-\sigma_x n - \sigma_y m) \tag{3}$$

In principle, the couplings between the neighboring waveguides is also affected by the chirp. However, if the chirp in the refraction index varies slowly in space, then in the first-order approximation the waveguide couplings is affected in the same way:

$$V_{(n,m),(n+1,m)} = V_0 \exp(-\sigma_x n - \sigma_y m) = V_{(n,m),(n,m+1)}$$

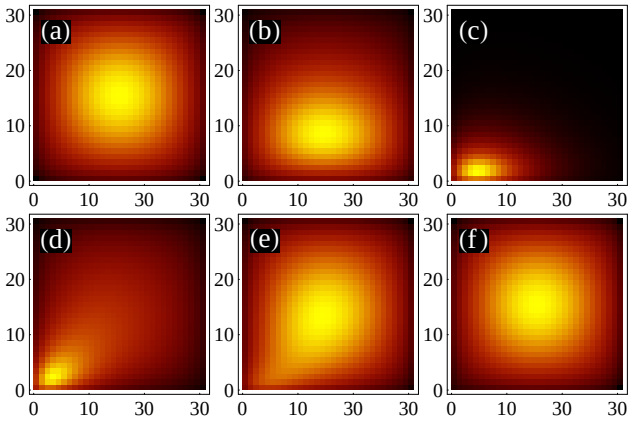

FIG. 2: Density profiles of localized nodeless mode for different values of the chirp (σ_x, σ_y) for $\lambda_0/V_0 = 1$. (a): $(0,0)$, (b) $(2\times10^{-4}, 3\times10^{-3})$, (c) $(3\times10^{-2}, 3\times10^{-1})$, (d) $(2\times10^{-1}, 5\times10^{-1})$, (e) $(10^{-1}, 1)$, (f) $(1,1)$. Anisotropic chirp in the propagation constant only.

$$V_{(n,m),(n-1,m)} = V_0 \exp(-\sigma_x(n-1) - \sigma_y m)$$

$$V_{(n,m),(n,m-1)} = V_0 \exp(-\sigma_x n - \sigma_y(m-1))$$

However, since the coupling between the waveguides also depends upon an overlap of the mode fields, it is possible in principle to alter the waveguide spacing judiciously in order to compensate for the spatial variation of the refraction index, rendering the couplings nearly constant: $V_{\mathbf{n},\mathbf{m}} \approx V_0$. Hereafter, we consider both the cases separately.

III. LINEAR SURFACE MODES

A. Chirp in the propagation constant

Equations for the stationary modes have the form,

$$\begin{aligned}\beta C_{n,m} &= \lambda_0 \exp(-\sigma_x n - \sigma_y m)\ C_{n,m} \\ &+ V_0 \sum_{j=\pm1} (C_{n+j,m} + C_{n,m+j}) + \gamma |C_{n,m}|^2 C_{n,m},\end{aligned} \tag{4}$$

We start by examining the $N \times N$ linear modes ($\gamma = 0$), relevant to the case of weak input power $\sum_{n,m} |C_{n,m}|^2 \ll 1$. For a fixed number of waveguides, we diagonalize the system of discrete linear equations (4) and find all the modes. In particular, we focus on the nodeless (fundamental) mode, and how it changes as a function of the chirp parameters σ_x and σ_y.

From Eq. (4) we find that, in the limit of large chirp, $\sigma_x, \sigma_y \gg 1$, the system reduces to a two-dimensional lattice with a linear impurity at one of the corner sites. It can be proven [17] that in this case for $N \to \infty$ a localized mode centered at the corner site is possible, provided

$$\lambda_0/V_0 > [2 - (16/3\pi)]^{-1} \equiv (\lambda_0/V_0)_c.$$

Thus, there appear two regimes: (1) For $\lambda_0/V_0 > (\lambda_0/V_0)_c \sim 3.3$, an increase in the chirp values shifts the center of the nodeless mode from the center of the lattice towards the corner site. For sufficiently large average chirp, $< \sigma >= (1/2)(\sigma_x + \sigma_y)$, the mode center approaches the corner site position and its spatial extension reduces considerably (see Fig. 1). (2) When $\lambda_0/V_0 < (\lambda_0/V_0)_c$, the mode center shifts from the center of the lattice towards the corner site upon the average chirp increase as above, but upon further chirp increase, the mode center shifts away from the corner site and it approaches the center of the lattice asymptotically (see Fig. 2).

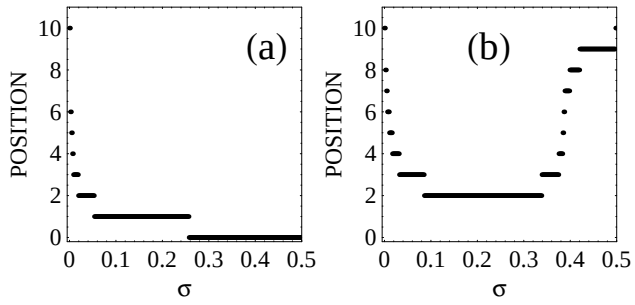

FIG. 3: Distance of the mode maximum from the corner of the array as a function of the chirp parameter, for the isotropic case $\sigma_x = \sigma_y \equiv \sigma$. (a): $\lambda_0/V = 5$. (b): $\lambda_0/V = 1$.

In order to visualize and quantify this behavior of the mode center as the chirp is increased, we consider the isotropic case $\sigma_x = \sigma_y$ and calculate numerically the mode position relative to the lattice corner along the diagonal (n, n) as a function of the chirp for both the cases, $\lambda_0/V_0 > (\lambda_0/V_0)_c$ and $\lambda_0/V_0 < (\lambda_0/V_0)_c$. The results are shown in Fig. 3. The observed dependence is presented by a series of discrete steps of a widely varying width. At small chirp, the fundamental mode is confined well inside the lattice and a small change of the chirp can alter the position of the mode maximum considerably. As the mode gets closer to the corner, the steps increase in size. For $\lambda_0/V_0 > (\lambda_0/V_0)_c$, the mode finally reaches the corner site where it will remain upon further chirp increase see Fig. 3(a)]. On the contrary,

for $\lambda_0/V_0 < (\lambda_0/V_0)_c$, the mode reaches a minimum distance from the corner and, upon further chirp increase, it shifts away from the corner and reaches the middle of the lattice in the limit of very large chirp [see Fig. 3(b)].

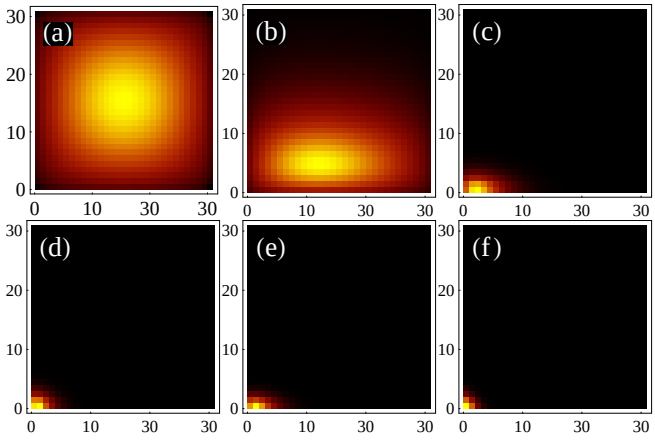

FIG. 4: Same as in Fig.2 but including chirp in propagation constant *and* in waveguide couplings.

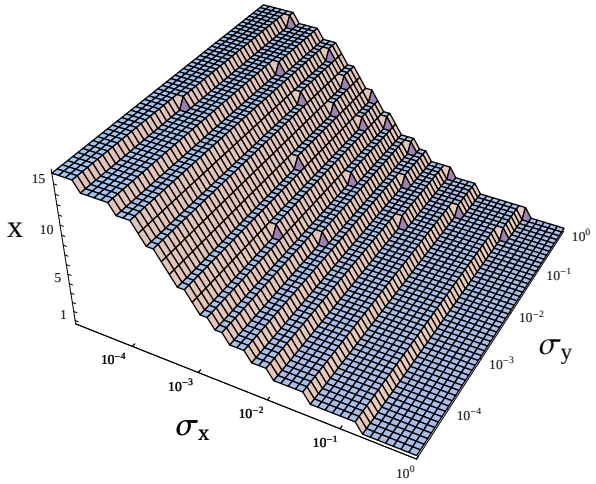

FIG. 5: Position of the center of the nodeless mode along the x-coordinate as a function of the chirp parameter for $N = 21$ and $\lambda_0/V_0 = 1$. The case of an anisotropic chirp in both the propagation constant and couplings.

B. Chirp in the propagation constant and waveguide coupling

This seems to be more realistic case that originates from modulation of the refractive index imposed on the periodic square array of coupled waveguides. If the modulation is smooth, then both the propagation constants and waveguide couplings are affected in the same manner. This leads to the following set of coupled equations for the linear modes:

$$\beta C_{n,m} = e^{-\sigma_x n-\sigma_y m}[\lambda_0 C_{n,m} + V_0(C_{n+1,m} + C_{n,m+1})] + V_0 e^{-\sigma_x n-\sigma_y m}[e^{\sigma_y} C_{n,m-1} + e^{\sigma_x} C_{n-1,m}]. \quad (5)$$

where $C_{n',m'} = 0$ if either $n' < 0$ or $m' < 0$.

In this case, from Eq. (5) we obtain that, in the limit of a large average chirp, the system becomes an effective trimer. Thus, the localized nodeless mode remains in the immediate vicinity of the corner site, and there will not be any bouncing phenomena for the mode center as in the previous section.

As the values of the chirp in both directions are increased from zero, the fundamental mode will shift from the center of the lattice approaching the corner site, as shown in Fig. 4. The precise route of the mode center towards the corner site depends on the values of both σ_x and σ_y. We now perform a numerical sweep in the (σ_x, σ_y) space and record the position (x, y) of the mode maximum. The results for the x-position are shown in Fig. 5

Due to symmetry, the position of the y-coordinate of the mode maximum can be obtained from the same figure by exchanging σ_x and σ_y. We notice that, at small average chirp value, the mode center is very sensitive to the precise value of the chirps. As chirps are increased, the position of the mode center becomes less sensitive and the width of the 'terraces' become larger. For chirp values greater than, say ≈ 0.3, the mode will be centered on the corner site and will remain there upon further chirp increase.

IV. SURFACE SOLITONS IN CHIRPED NONLINEAR LATTICES

Having examined the main features of the fundamental linear (i.e., low power) surface modes in the presence of an anisotropic chirp, we now consider the case of a nonlinear lattice, i.e. $\gamma \neq 0$. We focus on the more interesting case examined in the previous section and, for a given value of β, we find nonlinear localized states by solving the stationary equations

numerically with the help of a straightforward extension of the multidimensional Newton-Raphson method used earlier in our analysis of the one-dimensional system [9]. To do so, we first present the two-dimensional $N \times N$ system as an effective, N^2-long one-dimensional chain by means of a convenient relabeling of the site coordinates, and then apply the usual Newton-Raphson method [9].

As an example, we consider the linear modes presented in Figs. 4(a-f) and recalculate them in the case of nonlinear lattice for $\gamma = 1$. The corresponding results for the nonlinear localized modes are shown in Figs. 6(a-f). We note that, in comparison with the linear modes, the position of the nonlinear mode center does not change, but the spatial extension of the mode is reduced considerably, due to the self-trapping effect.

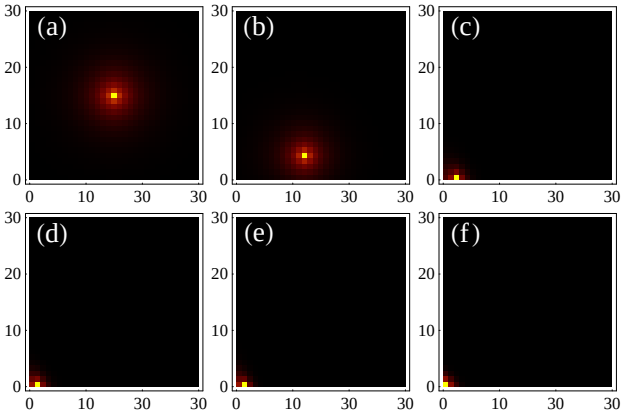

FIG. 6: Nonlinear localized modes near the corner of a two-dimensional lattice in the case of an anisotropic chirp in both the propagation constant and couplings. Parameters are the same as in Fig. 4 but for $\gamma = 1$.

Finally, we calculate the minimum power needed to create a nonlinear localized mode at the corner site, for given values of the chirp parameters (σ_x, σ_y). As we have might easily conjecture, at small average values of the lattice chirp, the minimum power is needed to create a stable mode while above a certain value of the chirp, no minimum power is required, similar to the case of a one-dimensional chirped lattice [9]. Figure 7 shows that this is indeed the case.

Therefore, by changing either the lattice chirp or the effective nonlinearity, we can control not only the mode localization but also its location in the lattice near the surface. This property provides an efficient physical mechanism for the low-power generation of nonlinear

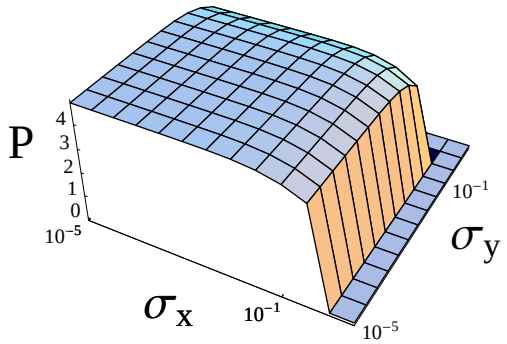

FIG. 7: Minimum power for creating a nonlinear localized surface mode at the lattice corner, as a function of the chirp parameters (σ_x, σ_y) for $\lambda_0/V = 1$. The case of an anisotropic chirp in both the propagation constant and couplings.

localized modes near lattice surfaces and other defects, where the threshold power for the generation of nonlinear localized mode is lower than in a bulk. It is now possible to move the localized mode in a given direction up to a desired position on the lattice by engineering both, the value and direction of the lattice chirp, and then localize the mode by further increasing the nonlinearity. As a matter of fact, this simple mechanism is presented in Figs. 4(a-f) and Figs. 6(a-f).

V. CONCLUSIONS

We have analyzed the properties of surface modes and discrete surface solitons in two-dimensional chirped linear and nonlinear photonic lattices, in the framework of an effective two-dimensional discrete model. We have demonstrated that the lattice chirp can change dramatically the conditions for the mode localization near the surface, and we have found numerically the families of linear surface modes and discrete surface solitons. We have demonstrated that, by manipulating the lattice chirp, we can control not only the mode localization but also its location in the lattice near the surface, and thus provide an efficient tool for the low-power generation of nonlinear localized modes and their control in realistic physical systems. We believe the basic principles of engineering the localization of linear and nonlinear localized modes in chirped lattices can be useful for their implementation in other discrete nonlinear systems.

VI. ACKNOWLEDGEMENTS

This work has been supported by Fondecyt grants 1050193 and 7050173 in Chile, and by the Australian Research Council in Australia. M.I.M. thanks ICFO-Institut de Ciencies Fotoniques (Bercelona) and the Nonlinear Physics Center at the Australian National University for hospitality and support.

[1] P. Yeh, A. Yariv, and A.Y. Cho, Appl. Phys. Lett. **32**, 102 (1978).

[2] K.G. Makris, S. Suntsov, D.N. Christodoulides, G.I. Stegeman, and A. Haché, Opt. Lett. **30**, 2466 (2005).

[3] S. Suntsov, K.G. Makris, D.N. Christodoulides, G.I. Stegeman, A. Haché, R. Morandotti, H. Yang, G. Salamo, and M. Sorel, Phys. Rev. Lett. **96**, 063901 (2006).

[4] M.I. Molina, R.A. Vicencio, and Yu.S Kivshar, Opt. Lett. **31**, 1693 (2006).

[5] Y.V. Kartashov, V.A. Vysloukh, and L. Torner, Phys. Rev. Lett. **96**, 073901 (2006).

[6] C.R. Rosberg, D.N. Neshev, W. Krolikowski, A. Mitchell, R.A. Vicencio, M.I. Molina, and Yu.S. Kivshar, Phys. Rev. Lett. **97**, 083901 (2006).

[7] E. Smirnov, M. Stepić, C. E. Rütter, D. Kip and V. Shandarov, Opt. Lett. **31**, 2338 (2006).

[8] Y.V. Kartashov, V.A. Vysloukh, and L. Torner, Phys. Rev. A **76**, 013831 (2007).

[9] M.I. Molina, Y.V. Kartashov, L. Torner, and Yu.S. Kivshar, Opt. Lett. **32**, 2668 (2007).

[10] Y. V. Kartashov and L. Torner, Opt. Lett. **31**, 2172 (2006)

[11] Y.V. Kartashov, V.A. Vysloukh, D. Mihalache, and L. Torner, Opt. Lett. **31**, 2329 (2006).

[12] K.G. Makris, J. Hudock, D.N. Christodoulides, G.I. Stegeman, O. Manela and M. Segev, Opt. Lett. **31**, 2774 (2006).

[13] H. Susanto, P.G. Kevrekidis, B.A. Malomed, R. Carretero-Gonzalez, and D.J. Frantzeskakis, Phys. Rev. E **75**, 056605 (2007).

[14] R.A. Vicencio, S. Flach, M.I. Molina, Yu.S. Kivshar, Phys. Lett. A **364**, 274 (2007).

[15] X. Wang, A. Bezryadina, Z. Chen, K. G. Makris, D. N. Christodoulides, and G. I. Stegeman, Phys. Rev. Lett. **98**, 123903 (2007).

[16] A. Szameit, Y. V. Kartashov, F. Dreisow, T. Pertsch, S. Nolte, A. Tünnermann, and L. Torner, Phys. Rev. Lett. **98**, 173903 (2007).

[17] M. I. Molina, Phys. Rev. B **74**, 045412 (2006).